NUMERICAL STUDY OF A DC ELECTROMAGNETIC LIQUID METAL PUMP: LIMITS OF THE MODEL

Nedeltcho Kandev
Institut de recherche d'Hydro-Quebec (IREQ) Quebec, Canada
600, av de la Montagne, Shawinigan, Quebec, G9N 7N5, Canada
kandev.nedeltcho@ireq.ca

Abstract This work presents the results of a 3D numerical magneto-hydrodynamic (MHD) simulation of an electromagnetic DC pump for liquid metal using a rectangular metal flow channel subjected to an externally imposed transversal inhomogeneous magnetic field. In this study, 3D numerical simulation based on the finite element method was carried out using the computer package COMSOL Multiphysics 3.5a. For this simulation, the liquid aluminum is used as an electrically conductive fluid. The application and the limits of the electromagnetic and the hydrodynamic models are discussed herein. The results of two typical examples are summarized here, including brake flow and pumping conditions for both laminar and turbulent metal flow. These simulations accurately represent the formation of an M shaped velocity profile of liquid metal under the influence of the imposed non-uniform magnetic field and are consistent with the results of recently published experimental and theoretical works.

Keywords: DC magnetic pump, MHD flow, finite element method.

1. Introduction

The concept of electromagnetic pumping of liquid metals was developed in the nineteen seventies first for zinc and aluminum and later for other molten metals. Electromagnetic pumps have many advantages over mechanical pumps including precise metal flow control without any moving parts, reduced energy consumption and less dross formation. A well-known example of the industrial applications of the EMP principle is the electromagnetic brake used in the continuous casting of large steel stabs to suppress the liquid metal motion within the mold. Another example of possible industrial application is as a velocity-meter for molten metal by measuring the Lorentz braking force [Thess, Votaykov and Kolesnicov (2006)].

Two different concepts of electromagnetic pumps for molten metals have been developed over the last forty years: a) a linear induction electromagnetic (AC) pump and b) a direct current (DC) electromagnetic pump. The most frequently used is the linear induction EM pump. The main advantage of this AC concept is that no direct contact with the molten metal is necessary. However, the linear induction AC pump can transfer a molten metal just horizontally without any metal head. The direct current (DC) electromagnetic principle has been used mainly to develop electromagnetic micro-pumps for biomedical and chemical applications for precise control of small volume of fluids in micro-channels [Jaime H. L. Parada and B.J. William (2007), Pei-Jen Wang, Chia-Yuan Chang and Ming-Lang Chang (2004) and Jang J. and S. S. Lee (2000)]. Our recent investigation [N.P. Kandev V. Kagan and A. Daoud (2010), A. Daoud and N.P. Kandev (2008)] showed that the DC electromagnetic pump can be used successfully in many liquid metal environments such as extrusion billet casting, metal refinery for transporting molten metals at different heads, alloys production etc. Electromagnetic DC pumps for aluminum with capacity up to 30 T/h were developed in 2008 and commercialized in the USA for different industrial applications.

The geometry of the MHD model considered in this work is shown schematically in Figure 1. A rectangular flat channel with electrically and thermally insulated boundaries is filled with liquid metal and submitted to a transversal magnetic field B_z varying along the x and y axes. This non uniform magnetic field can be simulated by using two permanent magnets on the bottom and top walls as shown in Figure 1 or, by using a 3D parametric function to impose the space dependent variables $B_z(x)$ and $B_z(y)$ inside the rectangular flat channel. A pair of electrodes is introduced on the vertical lateral walls of the channel at a right angle to the magnetic field. They supply an external electrostatic field E_e with desired magnitude and direction in the molten metal. The axial horizontal plane $(x - y)$ of the

channel (at z = 0) is in the half distance of the magnetic gap.

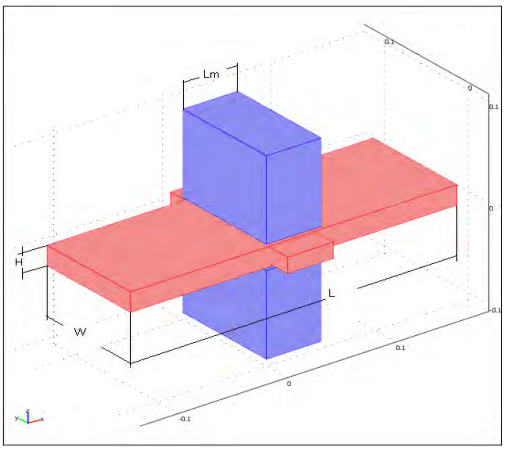

Figure 1. Simplified schema of the MHD model. Channel length L = 0.3 m, height H = 0.02 m and width W = 0.1 m. Magnet length Lm = 0.05 m [N.P. Kandev V. Kagan and A. Daoud (2010)]

The present complex MHD problem involving turbulences and a strongly inhomogeneous magnetic field is not necessarily symmetrical and, therefore, only a fully 3D high resolution simulation could grasp all spatial aspects of the electromagnetic and fluid dynamics phenomena.

The direct numerical simulation (DNS) would be the best physical approach for treating these MHD problems, especially for the boundary layers regions reduced to very small scales permitting the highest resolution. However, in many a DSN is not the ideal solution since it requires enormous time resolution and memory space.

Other numerical approaches mentioned in recent works [Votaykov and Zienicke (2007)] are Large eddy current simulations (LES) and Reynolds averaged stress models (RASN). These numerical approaches should be capable of catching turbulent features of the flow for the Hartmann layers near the boundaries, however the application of these approaches for inhomogeneous magnetic fields proves that there are still serious technical difficulties.

The usual theoretical formulation of the magneto hydrodynamic model for electrically conducting and Newtonian incompressible fluid has been derived from Ohm's law for moving media, coupled with the Navier-Stokes equations for laminar flow with Lorentz force given by the cross product $\vec{F}_L = \vec{J} \times \vec{B}$. The equations used for the 3D MHD model can be summarized as follows:

1. Electromagnetic part of the problem

$$\vec{J} = \sigma(-\nabla\phi + \vec{u} \times \vec{B}) \quad (1)$$

$$\nabla \cdot \vec{J} = 0 \quad (2)$$

2. Fluid dynamics for laminar flow

$$\rho \frac{\partial \vec{u}}{\partial t} = -\nabla P + \eta\rho\nabla^2\vec{u} + \vec{F}_L \quad (3)$$

$$\nabla \cdot \vec{u} = 0 \quad (4)$$

The electromagnetic part of the problem is presented by Ohm's law in equation (1) whereby the electrical scalar potential ϕ has to be determined by solving the Poisson equation: $\nabla^2\phi = \nabla \cdot (\vec{u} \times \vec{B})$. Here $\vec{u}$ is the velocity of the fluid, $\vec{J}$ is the current density and σ is the electrical conductivity. Equation (2) denotes the conservation of the electrical current.

Habitually, the external non-uniform magnetic field B is simulated by using a 3D parametric function to impose the space-dependent variables $B_z(x)$ and $B_z(y)$ inside the rectangular flat channel. An example of such 3D function with maximum value of $B_z(x=0, y=0)$ = 0.7 T is given in Figure 2.

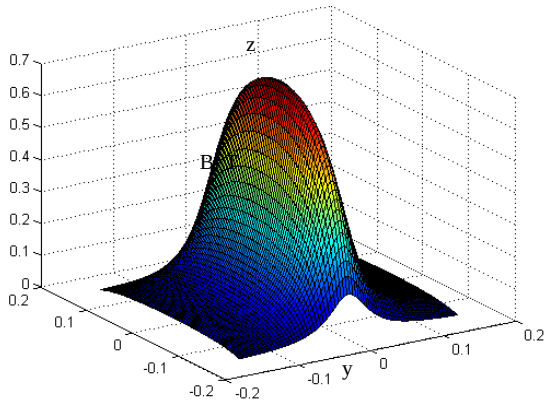

Figure 2. Example of 3D function simulating an externally imposed inhomogeneous magnetic field B

The problems are solved using stationary formulation for the electromagnetic part with induced Lorentz current density term in the moving medium (the induced current does not move with the moving medium and does not produce magnetic field). This *"quasi-static"* approximation is valid under the assumption that the induced magnetic field is infinitely small in comparison to the externally imposed magnetic field.

Our previous studies [N.P. Kandev, V. Kagan and A. Daoud (2010)] showed that this assumption is absolutely acceptable for the classical "brake–flow" case, where the maximal magnetic field generated by the induced currents is smaller by a factor of about 10^{-5} in comparison to the external magnetic field.

The fluid dynamics part of the problem is determined by equation (3) representing the conservation of momentum of the fluid in motion, where P denotes the pressure, ρ is the density and the η is the kinematic viscosity of the fluid, where the conservation of mass is given in equation (4). The coupling between the electromagnetic model and the fluid model is achieved by introducing the Lorentz force F_L as a body force in the conservation of momentum and the use of the fluid velocity, calculated by the fluid model, in Ohm's law.

The above described model can provide a satisfactory solution for the laminar brake–flow case only, not for the electromagnetic pumping case.

2. Numerical modeling

In our simulations we have used the computer package Comsol-Multiphysics which is based on the finite element method. The main advantage of using Comsol is that it is not necessary to write all internal source codes since the basic expressions are already built-in. Moreover, with Comsol it is possible to use coupling of different physical modules to carry out MHD simulations, for example: Magnetostatics, Conductive Media DC, Navier-Stokes flow model etc.

In this study, where the model must represent an actual pump for aluminum, working at different operating conditions, liquid aluminum at 700°C is used as an electrically conductive fluid with density ρ = 2385 kg/m^3, electric conductivity σ = 5e6 S/m and kinematic viscosity η = 0.545e-6 m^2/s.

In all simulated cases in this study the electromagnetic domain is delimited by an air sphere. On the external boundaries of this air domain the magnetic and electric conditions are fixed to: $\vec{n}\times\vec{A}=0$ and $\vec{n}.\vec{J}=0$, where $\vec{n}$ is a normal vector to the boundary. The interior boundaries between the permanent magnets system, the channel and the air assume continuity, corresponding to a homogenous Neumann condition. Electrically insulated boundaries of the channel in the presence of two electrodes on the vertical lateral walls of the channel at a right angle to the magnetic field are considered.

The problems are solved using a stationary segregated solver. This method of resolution was chosen because it was more stable than the fully coupled method (only one group of variables).

2.1 Laminar MHD flow

The first case involves simulating a low laminar channel flow at relatively low magnetic field and without any external DC current ($\vec{J}_e=0$). The goal of this simulation is to validate the MHD brake flow hypothesis at a low Reynolds number and to compare these results with those of other similar published works.

The formulation of this model in Comsol has been derived from the Maxwell-Ampere equation, also using Ohm's law, coupled with the Navier-Stokes equations for laminar flow with Lorentz force $\vec{F}_L=\vec{J}\times(\nabla\times\vec{A})$ by introducing the magnetic vector potential $\vec{A}$ where $\vec{B}=(\nabla\times\vec{A})$.

$$\nabla\times\left(\frac{\nabla\times\vec{A}}{\mu}\right)=\sigma(-\nabla\phi+\vec{u}\times(\nabla\times\vec{A})) \qquad (5)$$

$$\vec{J}=\sigma(-\nabla\phi+\vec{u}\times(\nabla\times\vec{A})) \qquad (5\text{-a})$$

$$\nabla\cdot\vec{J}=0 \qquad (6)$$

$$\rho(\vec{u}\cdot\nabla)\vec{u}-\nabla\cdot\left[\eta\left(\nabla\vec{u}+(\nabla\vec{u})^T\right)\right]=-\nabla P+F_L \qquad (7)$$

$$\nabla\cdot\vec{u}=0 \qquad (8)$$

Here Maxwell-Ampère's law in equation (5) includes Ohm's law (5-a). The constants in equations (5) are the electrical conductivity σ and the permeability μ. Here the space dependent variables are $\vec{A}(x, y, z)$, $\vec{J}(x, y, z)$ and $\phi(x, y, z)$.

Coupling of the Magnetostatics (emqav), and Incompressible Navier-Stokes (chns) laminar models is used to carry out this simulation. The coupling between the electromagnetic model and the fluid model is achieved by introducing the Lorentz force F_L as a body force in the conservation of momentum and the use of the fluid velocity, calculated by the fluid model, in Ohm's law.

The MHD effect depends on the electrical conductivity, the density and the viscosity of the liquid metal. It is characterized by the Hartmann number $H_a=B_0 h\sqrt{\sigma/\rho\eta}$, and by the interaction parameter $N=H_a^2/R_e$. Here R_e is the Reynolds number, given by $R_e=U_0 h/\eta$, U_0 is the mean velocity of the liquid metal and B_0 is the mean magnetic flux density. The Hartmann and the Reynolds numbers are defined here with the half – height of the channel (h=H/2=0.01m).

For the example given below the boundary conditions of the fluid model are determined by the imposed inlet mean velocity U_o = 0.02 m/s, the mean magnetic flux density B_0 = 0.092 T and the outlet pressure P_{outlet} = 0. As result, the Reynolds number is *Re*= 367, the Hartmann number is *Ha* = 57 and the interaction parameter *N* = 8.85. "No-slip" velocity conditions were considered on the sides, top and bottom walls of the channel.

For this example, the shape of the externally imposed transversal magnetic flux density $B_z(x)$ along the *x* axis for *z* = 0 and *y* = 0 is plotted in Figure 2a. The velocity field in the central horizontal plane (z = 0) of the studied channel is given on Figure 2b.

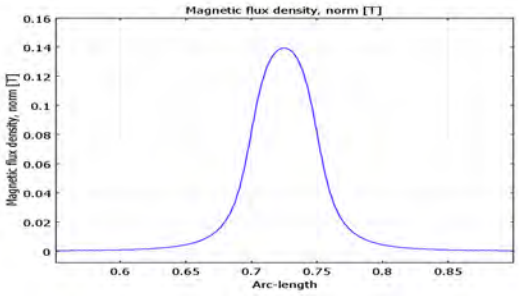

Figure 2a: Magnetic flux density $B_z(x)$ along the *x* axis for *z* = 0 and *y* = 0

The maximum magnetic flux density is 0.14 T and is located in the vertical axis of the magnetic gap. Notice that all MHD parameters are defined by the overall mean magnetic flux density B_0 = 0.092 T.

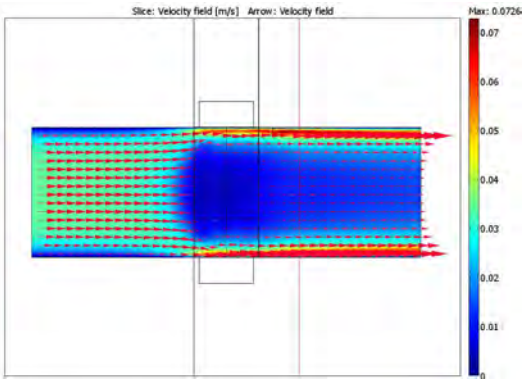

Figure 2b: Velocity field in the central horizontal plane (z = 0) of the channel. B_0 = 0.092 T, Re=367, N=8.85, U_0= 0.02 m/s.

The fluid velocity profile at different fixed positions along the *x*-axis in the central horizontal plane (z=0) of the channel $u_x(y)$ is shown in Figure 3.

These results show that under the opposite to the flow direction Lorentz force, the inlet laminar velocity profile is disturbed in the magnetic region, developing a typical M shape, which is a demonstration of MHD brake flow process.

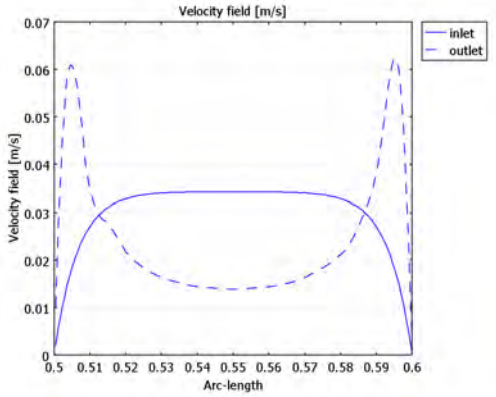

Figure 3: Fluid velocity profile $u_x(y)$ x-axis: Inlet laminar flow (solid curve), and outlet velocity (dashed curve)

This example shows that the simulation of laminar channel flow of liquid metal correctly represents the formation of an M shaped velocity profile and concurs with the results of recently published works [2, 3 and 4].

2.2 Turbulent MHD flow

As mentioned above, a turbulent structure has to be applied where the model simulates a real MHD pump working at high metal flow rate and high Reynolds number. To carry out this simulation with Comsol, a turbulent model instead of the laminar flow model, as well as a DC conductive media model must be added to simulate the external DC current producing the pumping Lorentz force.

Actually, three different models Magnetostatics (emqav), DC conductive media (emdc) and k-ε Turbulence model (chns) were coupled for this simulation.

The electromagnetic model, showed above in equations (5) and (6), was modified in terms of the electrical field intensity $\vec{E} = -\nabla\phi$, and externally applied electrical field intensity $\sigma\vec{E}_e = \vec{J}_e$ as follows:

$$\nabla\times\left(\frac{\nabla\times\vec{A}}{\mu}\right) = \sigma(\vec{E}+\vec{u}\times(\nabla\times\vec{A})) + \sigma\vec{E}_e \qquad (9)$$

$$\vec{J} = \sigma(\vec{E}+\vec{u}\times(\nabla\times\vec{A})) + \vec{J}_e \qquad (10)$$

$$\nabla\cdot\vec{J} = 0 \qquad (11)$$

Notice that in this case, the Lorentz force $\vec{F}_L = \vec{J} \times (\nabla \times \vec{A})$, introduced as a body force in the turbulent flow model, considers current intensity $\vec{J}$ as a vector sum of the internal $\sigma(\vec{E} + \vec{u} \times (\nabla \times \vec{A}))$ and the external $\vec{J}_e$ current density see equation (10). Actually, a DC electrical potential difference is applied in the (emdc) model between the two electrodes to impose an external electrostatic field E_e in the molten metal with desired magnitude and direction. In pumping operating conditions, the external electrostatic field $\vec{E}_e$ dominates the induced electromotive field and the resulting current is driven through the liquid metal in the positive *y*-direction, thus producing electromagnetic force acting in the direction of the flow.

The turbulent flow model is determined by equations (12), (13) and (14), representing conservation of momentum, turbulence kinetic energy (k) and dissipation rate (ε) of the fluid respectively. Equation (15) is used to calculate the kinematical turbulent viscosity (η_T) and equation (16) represents the conservation of mass.

$$\rho(\vec{u} \cdot \nabla)\vec{u} - \nabla \cdot \left[(\eta + \eta_T)\left(\nabla \vec{u} + (\nabla \vec{u})^T\right)\right] = -\nabla P + \vec{F}_L \qquad (12)$$

$$\rho \vec{u} \cdot \nabla k - \nabla \cdot \left[\left(\eta + \frac{\eta_T}{\sigma_k}\right)\nabla k\right] = \frac{1}{2}\eta_T\left(\nabla \vec{u} + (\nabla \vec{u})^T\right)^2 - \rho\varepsilon \qquad (13)$$

$$\rho \vec{u} \cdot \nabla \varepsilon - \nabla \cdot \left[\left(\eta + \frac{\eta_t}{\sigma_\varepsilon}\right)\nabla \varepsilon\right] = \frac{1}{2}C_{\varepsilon 1}\frac{\varepsilon}{k}\eta_T\left(\nabla \vec{u} + (\nabla \vec{u})^T\right)^2 - \rho C_{\varepsilon 2}\frac{\varepsilon^2}{k} \qquad (14)$$

$$\eta_T = \rho C_\mu \frac{k^2}{\varepsilon} \qquad (15)$$

$$\nabla \cdot \vec{u} = 0 \qquad (16)$$

The constants are fixed as follows: C_μ=0.09, $C_{\varepsilon 1}$=1.44, $C_{\varepsilon 2}$=1.92, σ_k=1 and σ_ε=1.3. In this case of turbulent flow, two groups of dependent variables are chosen: the first group includes the fluid velocity components *u(x,y,z)* and the pressure *P(x,y,z);* the second group includes the turbulence components (*log(ε)* and *log(k)).*

The main advantage of using this complex k-ε Turbulence model built into Comsol Multiphysics is that the solving algorithms are optimized and the model coefficients have been tuned by computer optimization using available experimental data.

The domain of the flow is given by a rectangular flat channel shown in Figure 1. In the case of turbulent flow, the inlet and outlet fluid boundary conditions are $P=P_{inlet}$ and P_{outlet}=0 respectively. A logarithmic wall function is applied as a boundary condition for the channel walls to represent the turbulent boundary layer.

As an example, DC potential difference of 0.36V was imposed between the electrodes, thus generating external currents of 1794A.

Notice that in this case the magnetic field is about five times greater (B_0 = 0.46 T with maximum of 0.7 T) than that of the laminar flow case.

The boundary conditions of the fluid model are determined by the imposed inlet constant pressure P_{inlet}= -17000 Pa and outlet pressure P_{outlet} = 0. This negative pressure represents the pressure drops as a function of the flow rate in the real metal transfer circuit used in previous aluminum pumping tests. It was determined by calculating the hydrodynamic losses of the experimental duct at mean flow rate of 0.88m/s [N.P. Kandev, V. Kagan and A. Daoud (2010)]. These imposed conditions generated a mean fluid velocity of 0.88 m/s, thus giving Reynolds number *Re*=16110, Hartmann number *Ha* = 280 and interaction parameter *N* = 5.05. The developed external electromagnetic force is 69.7 N and the internal Lorentz braking force F_{Lbr}= -38.93 N.

Figure 5 illustrates the shape of the velocity field in the central horizontal plane (z = 0) of the channel for this case and Figure 6 shows the fluid velocity profile at different positions along the *x*-axis $u_x(y)$.

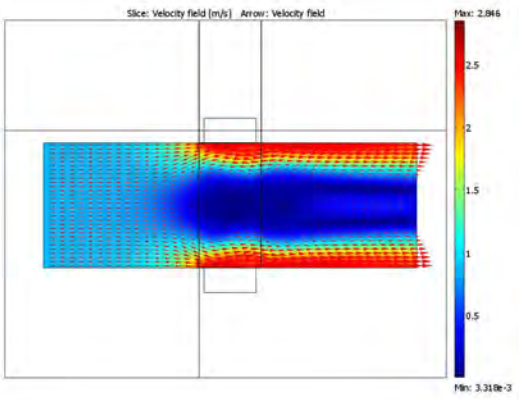

Figure 5: Vectors of the velocity field in the axial horizontal plane (z = 0) of the channel. B_0 = 0.46 T, Re=16110, N=5.05, U_0= 0.88 m/s.

The simulation results show that the MHD equilibrium is reached at a mean velocity of 0.88 m/s when the external DC electromagnetic driving forces F_e compensates completely the hydrodynamic losses of the fluid transfer circuit and the Lorentz braking force F_{Lbr} This result shows also a significant transformation of the originally developed turbulent flow profile into M or U chaps in the magnetic zone.

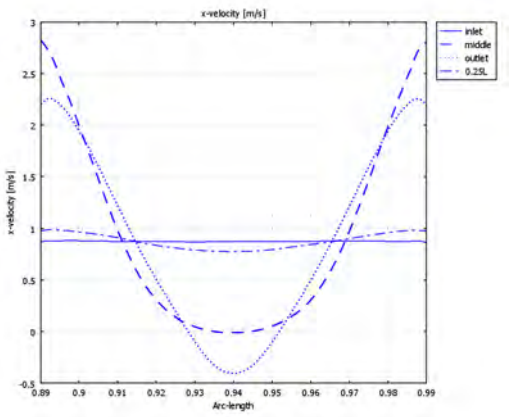

Figure 6: Fluid velocity profile on *y*-axis *u(y)* at different positions along the *x*-axis: Inlet flow (solid curve), 0.25 L from the inlet (dashed dotted curve), Middle (dashed curve) and Outlet velocity

The maximum to mean velocity ratio $FD = U_{max}/U_0$ in this case is 3.23, demonstrating a significant distortion of the inlet turbulent flow profile by traveling through the magnetic region. At a quarter of the distance from the inlet of the channel (0.25L), the velocity profile exhibits relatively low deformation, but it is completely distorted in the next quarter length by entering in the high magnetic field area. The vectors of the induced current density are plotted in Figure 7.

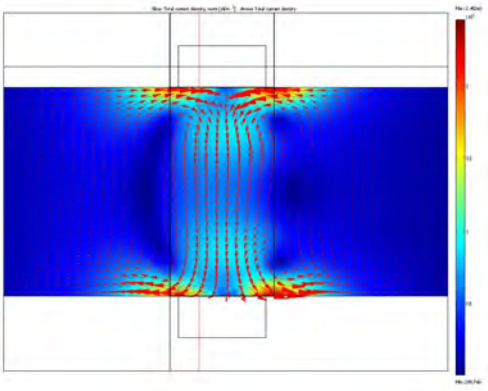

Figure 7: Induced current density in the liquid aluminum on the axial horizontal plane (z = 0)

The appearance of two couples of small current loops located on both side of the magnetic poles is evident. These amazing current "turbulences" are located in the zone of decreasing magnetic field where the electrical field changes its sign.

Figure 8 depicts the vectors of the total Lorentz force density in the axial horizontal plane (z = 0) of the channel. For this case the total electromagnetic driving force in the *x* direction is $F = F_e + F_{Lbr}$ =30.77 N.

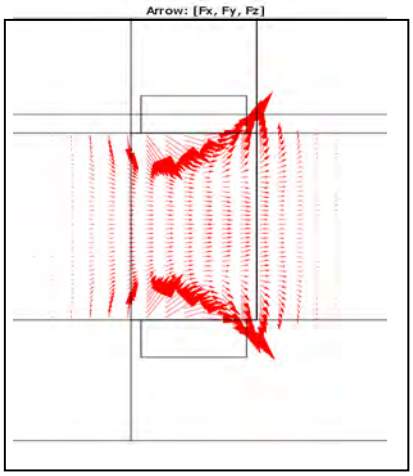

Figure 8: Vector plot of the total Lorentz force in the axial horizontal plane (z = 0)

This figure indicates that the electromagnetic driving force at high driving DC currents and high flow velocity is significantly non-uniform and is located in the magnetic region close to the lateral walls.

3. Conclusions

On the whole, the simulation of laminar and turbulent channel flow of liquid aluminum presented in this study accurately represents the formation of an M shaped velocity profile and corresponds with the results of recently published experimental and theoretical works [1, 2, 3 and 5].

For both laminar and turbulent flow cases the electromagnetic domain was delimited by an air sphere and the non-uniform magnetic field was simulated by using two permanent magnets fixed on the bottom and top walls of the channel and coupled by a steel yoke. This model utilizes not only Ohm's law, but also the Maxwell - Ampere equation, thus representing more precisely a real EM pump, especially for turbulent pumping conditions involving high driving DC currents and high flow velocity. Actually, for the turbulent pumping case, our fully 3D simulation revealed the appearance of two couples of small current loops located on both side of the magnetic poles ensuing from the complex spatial interaction of electromagnetic and hydrodynamic phenomena.

4. References:

1. Kandev N., V. Kagan and A. Daoud: Electromagnetic DC Pump of Liquid Aluminium: Computer Simulation and Experimental Study, *Journal of FDMP*, Vol. 6, No 3, pp. 291-318, 2010.

2. Votaykov Evgeny V., Egbert A. Zienicke: Numerical study of liquid metal flow in a rectangular duct under the influence of a heterogeneous magnetic field. *FDMP, vol.1,* pp 101- 117, 2007.

3. Parada Jaime H. L. and William B.J. Zimerman: Numerical simulation of a magnetohydrodynamic DC microdevice. *Multiphysics Modelling with Finite element methods University of Sheffield,U.K. Vol.18*, pp 375-391, 2007.

4. Jang J. and S. S. Lee: Theoretical and experimental study on MHD micro-pump. *Sens. Actuators A, Vol 80*, PP. 84-89, 2000.

5. Andreev O., Yu. Kolesnikov and A. Thess: Experimental study of liquid metal channel flow under the influence f a nonuniform magnetic field. *Phys Fluids, Vol 18, 065108*, 2006.

6. Holroyd Richard J.: An experimental study of the effects of wall conductivity, non-uniform magnetic field and variable-area ducts on liquid metal flow at high Hartmann number (Part 1: Ducts with non-conducting walls. *J. Fluid Mech, vol 93, part 4*, pp. 609-630, 1979.

7 Hughes M., K. A. Pericleous and M. Cross: The Numerical modelling of DC electromagnetic pump and brake flow. *Appl. Math. Modelling*, Vol 19, PP. 713-723, Dec. 1995.